Final Report

By

Ansel Higgs

Fadi Al Zuabi

Lance Pan

Final Report for ECE445, Senior Design, Fall 2018

TA: Evan Widloski

December 2018

Project No. 23

Abstract

This report focuses on the work done by the authors for their senior design project. The project consists of a DMX addressable fiber optic lighting system designed for an artwork located in the lobby of the University of Illinois at Urbana Champaign Electronic and Computer Engineering Building. The system comprises of 3 main parts: a control module, a lighting module, and a power module. Light is focused from high power LEDs through mounted lenses into the end of fiber optic cables that will then attach to the artwork. The work this semester resulted in a working product, but final aesthetic decisions have not yet been made and many improvements would make a full scale installation much more practical.

Contents

1. Introduction

To perform at today's standards, a proper lighting system must provide even illumination across its target while maintaining a discreet appearance. To tackle this challenge, we designed a modular, DMX addressable lighting system that uses fiber optic cables to create a precisely directed lighting solution intended for a specific piece of artwork. An important factor is the discreteness of the system as well as ensuring that the final aesthetic result is not overbearing but also effective enough to draw attention to the artwork. Figure 1 details the block diagram for our design.

1.1 Block Diagram

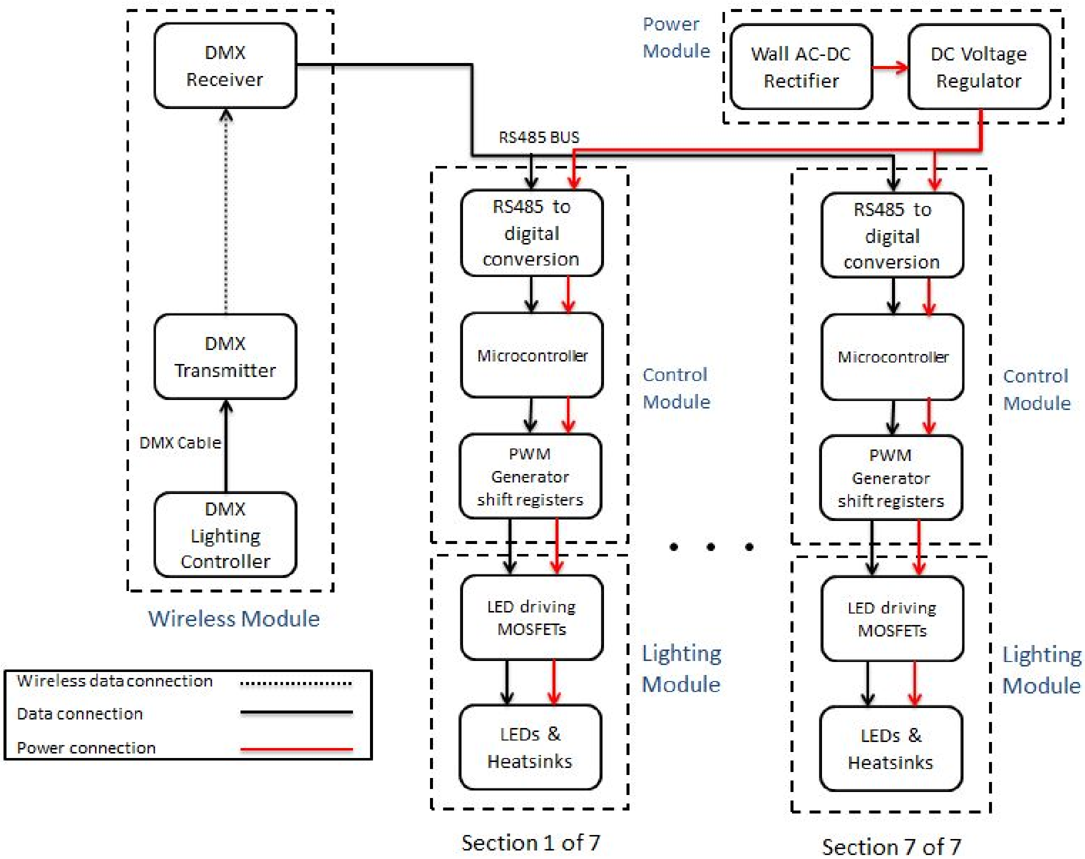

Figure 1 Block Diagram

2. Design

2.1 Signal Protocol

DMX (Digital Multiplexer) is a differential level asynchronous protocol most commonly used to control lighting fixtures. The protocol is broken up into the following: an idle period, a break period, a mark after break period, and a start frame followed by data frames separated by 2 high bits and 1 low bit to separate frames. Each frame contains a single byte of data, with the total number of frames going up to 512. Figure 2 illustrates the general format of the protocol. Note that the protocol transmits both this and an inverted version in order to ensure accuracy. We used one frame to control the intensity of one light for a total of 30 frames per module.

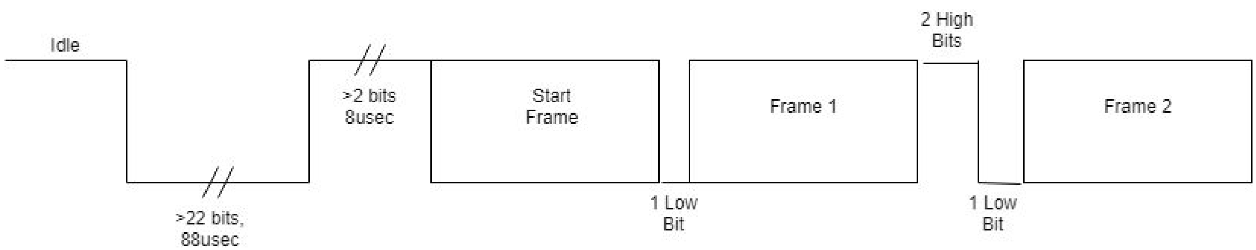

Figure 2 DMX Protocol Diagram

The DMX protocol proved to have several challenges, such as a highly variable idle period. The protocol defines the break period as at least 88 µs; the mark after break signal must have a minimum of high output for 8 µs [1]. To further complicate this, the wireless transmitter and receiver we purchased induce an extremely unpredictable variance to the timing of each packet. Careful consideration was taken in order to ensure that these variances would not lead to errors in interpretation.

2.2 PCB Layout

2.2.1 Trace Specification

Due to the relatively high power of the lighting module, careful consideration had to be taken for the design. The goal is to minimize resistance of the traces that carry power in order to ensure as little power waste as possible, as well as to maximize heat dissipation characteristics. Minimum trace widths were calculated using formulas from IPC-2221 [2] as is as follows:

$$Area\ [mils^2] = \left(\frac{Current\ [Amps]}{k*(Trise\ [C])^b}\right)^{1/c} \quad \text{[Eq. 1]}$$

$$Width\ [mils] = \frac{Area\ [mils^2]}{Thickness\ [oz] * 1.378\ [mils/oz]} \quad \text{[Eq.2]}$$

Given IPC-2221 defined external layers constants are defined as: k=0.048, b=0.44, c=0.725.

2.2.2 Control Module

For the control module the expected currents are all quite low, with the largest on the board being the current sink in the PWM outputs at approximately 15mA. Using equations 1 and 2 above, the minimum trace width is 0.160 mil with an ambient temperature of 25 ˚C and temperature rise of 20 ˚C. However, in the interest of minimizing resistance, the trace width used on the control board was generously oversized to 7.87 mils.

We discovered that the ATmega328P microcontroller our design uses does not have a very stable internal oscillator, with a 7.5% variance across the operating temperature range given a perfectly stable supply voltage [3]. This could potentially be a serious problem when used with serial communication, which our design has for both data input to the microcontroller and output to the PWM generators. In order to prevent this issue, a 20 MHz external crystal oscillator with a frequency stability of ±100 ppm was added to the design and connected to the microcontroller. Figure 3 shows the PCB layout for the control module. Note some connections are left open (such as the crystal oscillator output and the error outputs on the PWM drivers). This was done intentionally in order to allow for flexible testing and setup of the board.

2.2.3 Lighting Module

For the lighting module the maximum rated current per led is 1 Amp. Each lighting module has 8 LEDs so the total current would be ~8 A. Using the same conditions and equations 1 & 2, the minimum trace width per LED and in total are 7.77 mils and 137 mils respectively. In order to minimize resistance, the only traces on this board are the inputs from the outputs of the PWM generator which are oversized at 16 mils. For the rest of the connections, copper pour planes were used. This includes both a top and bottom plane for the ground connected by vias intended to reduce resistance as much as possible as shown in Figure 4.

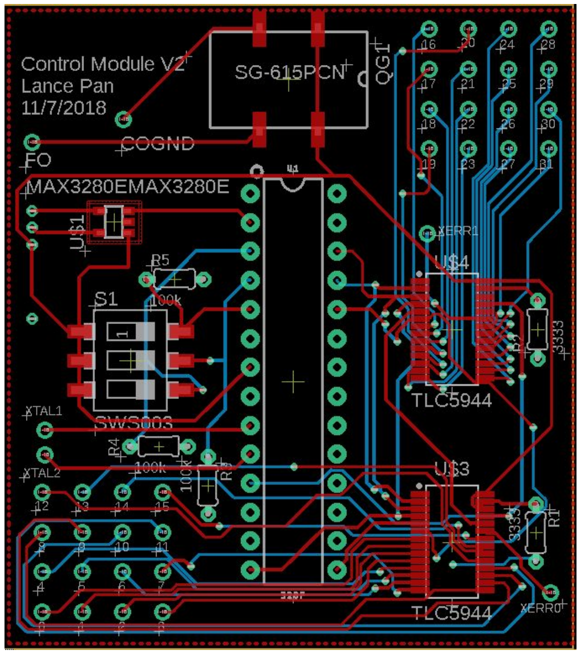

Figure 3 Control Module PCB Layout

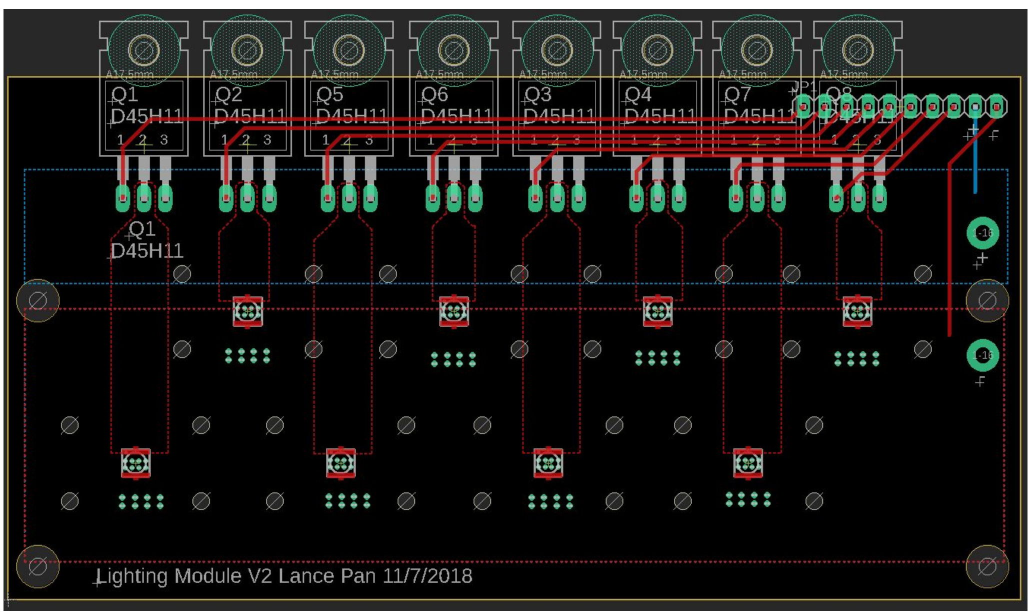

Figure 4 Lighting Module PCB Layout

2.2.4 Lighting Module Thermal Management

Another key design consideration is thermal management for the LEDs. The LED driving BJTs in out design are through hole mounted, so their thermal pads will be exposed to the air. This means that they should have a thermal resistance of 62.5 °C/W [12]. The LEDs are surface mount, so at the recommendation of the manufacturer, thermal vias were placed in the PCB underneath the LED thermal pads. Further testing revealed that thermal vias alone were not sufficient to dissipate heat during maximum LED intensity, so a heatsink and fan were mounted on the bottom of the lighting module with thermal paste to reduce resistance between the vias and sink.

2.3 Microcontroller

We are using the ATmega328p microcontroller to receive and process the DMX signal input and control the PWM generator chips to change the brightness of the LEDs according to the DMX data. The Atmega was chosen due to its number of I/O pins and reliable documentation.

2.3.1 USART0 Receiver

To receive the control input we used the Universal Synchronous Asynchronous Receiver Transmitter (USART0) on the ATmega328p. By specifying the variables of the USART0 to a BAUD rate of 200 kb/s, 8 data bits, 2 stop bits, and no parity, the microcontroller can receive the DMX data frame [3]. However, the USART0 does not inherently recognize the Start-of-Packet which is critical to receive the frames in order. We noticed that the start of packet looks like a frame, with one high start bit followed by more than 8 bits of data. This will trigger a frame error bit in one of the USART0 registers. Another difference between the Start-Of-Packet and a regular frame is that the stop bit will be high instead of low, so we changed the USART0 specification to receive 9 data bits instead of 8 and check the 9th bit to recognize the start of packet. The first byte (starting frame) of the DMX should always be 0x00, so after recognizing the start of packet we check if the start byte equals 0x00 then start receiving the frames in order. The flowchart in Figure 5 shows the start of packet algorithm.

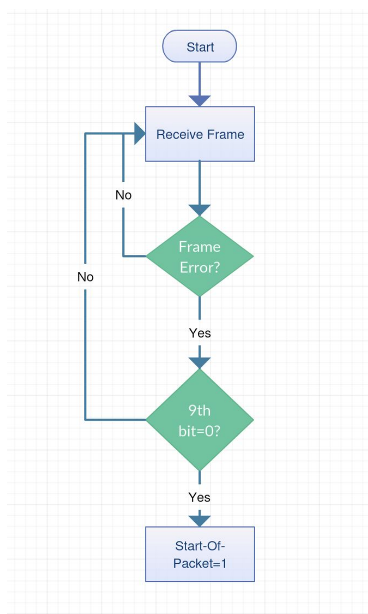

Figure 5 Start of Packet detection Flowchart

2.3.2 PWM Generator Control (TLC5944)

The TLC5944 chip outputs 16 constant current sinks. Each output value is set by the values of two registers, the 6-bit Dot Correction register (DC) and the 12-bit Grayscale register (GS). Both registers set the percentage of the current to be sunk. The difference is that DC is used to permanently limit the current to an output, while GS is better used to change the brightness. Both must be set at the start for the TLC5944 to work. To control and run the TLC5944, the microcontroller needs to manage three parts of the TLC5944 chip: setting Dot Correction data, setting Grayscale data, and run the chip using GSclk and Blank pins. Dot Correct currently initializes at 100% as we want to drive all LEDs up their maximum intensity. [13]

The Grayscale register is continuously updated with the DMX data. The microcontroller processes and shifts the DMX frame into the GS registers once received and latches all the registers to set the outputs once the 32 frames are received. This allows faster control compared to storing the frames and then shifting them out. To run the TLC5944 outputs, GSclk needs to run the GS counter that counts from 0 to 4095 and the microcontroller must toggle Blank every 4096 count to reset the counter. This created some complication as we were running GSclk by toggling the I/O pin 4096 times and then toggling Blank between receiving the control signal. This caused the LEDs to rapidly blink due to the time delay caused by the slow transmission of the DMX (250 kb/s). To solve this issue we used two features of the ATmega328p: Timer/Counter 0 to generate GSclk and Timer/Counter1 with interrupts to toggle Blank. Timer/Counter 0 is set to generate a clock at 10 MHz (½ of the system clock) for the GSclk. Timer/Counter 1 counts to 4096 and launches an interrupt routine that toggles Blank to reset the GSclk. This method solved the issue and now the TLC5944 always runs independently from setting DC and GS values. This method also allows the TLC5944 to keep running with the previously set values even if the DMX receiver is disconnected. Figure 6 details this process in a flowchart form.

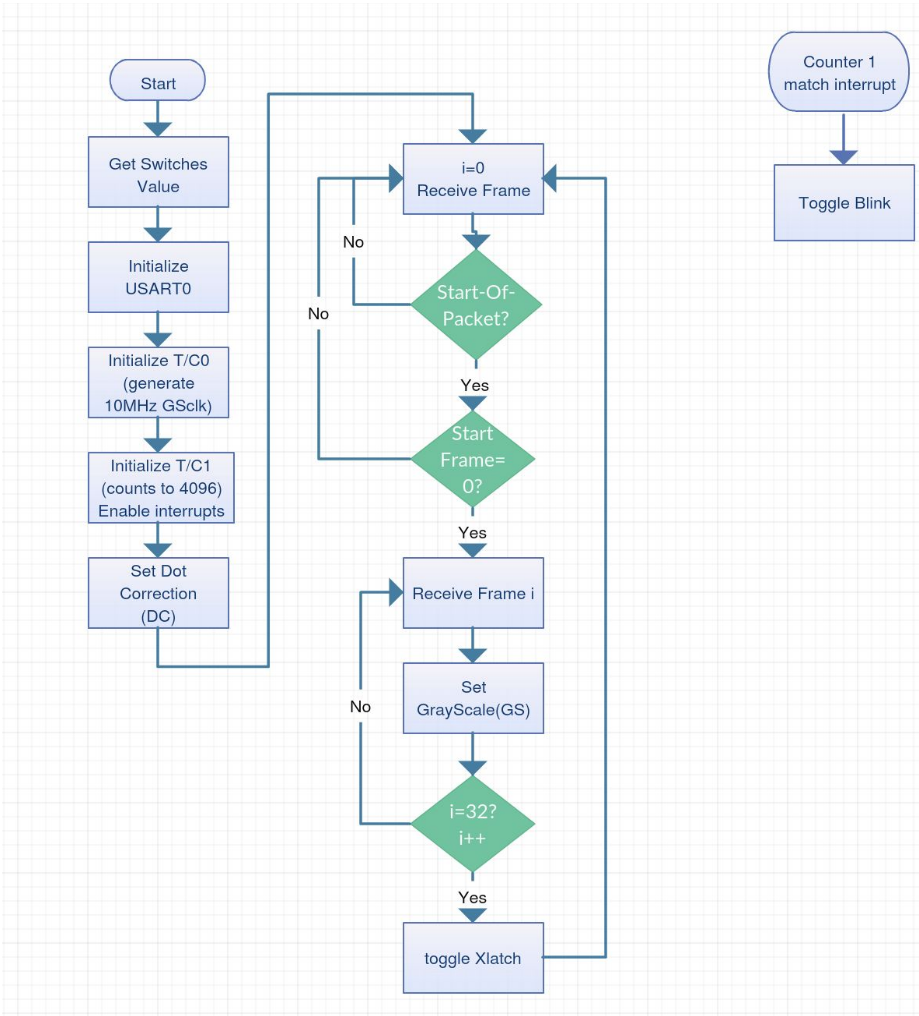

Figure 6 Program Flowchart

2.4 Fiber Optic Lighting Element

2.4.1 Fiber Optic Cables

Due to the aesthetic nature of the project, we tested several fiber optic configurations to illuminate various setups of tubes in the artwork. There are currently two main competing options: a single large fiber optic end glow cable and a bundled strand of smaller fiber optic cables. As our design uses a series of lenses mounted on the LED in order to focus down the light to ~7mm diameter circle we have aimed to have cabling with a similar diameter in order to maximize light transfer from LED to the fiber optic cable(s). A single large fiber optic would offer more efficiency in light transfer from LED to cable, but less options to disperse light over a larger area. A stranded fiber optic cable would offer more options for lighting, such as spreading out the individual strands throughout the artwork in order to attain a more even lighting. However, a stranded fiber optic cable runs into the inherent issue of packing circles within circles.

Given a desired total cable diameter being ~7mm we can use the ratio of the outer to inner circle diameter in order to determine highest possible packing factor. For example, a very high ratio of outer to inner circle diameter will result in a very high packing factor. However, this is not necessarily practical as the strands generally are sold in single lengths and as a result it is impractical to bind the much larger number of strands together. 0.75mm diameter fiber optic cable required too many cables in order to attain the desired cable thickness, so 1.5mm diameter fiber optic cable was determined as the next option to test. The ratio of the outer to inner diameter for 1.5 mm diameter fiber optic cable is 4.67, which is most closely attained with 16 strands with a ratio of outer to inner diameter of 4.615 [4] as shown in Figure 7. This has an optimal packing factor of 0.7512, which means that there will be a minimum of 25% inherent light loss due to the inefficient packing. As the inner cable diameter increases, this packing factor decreases. For example, a 2 mm diameter cable yields a diameter ratio of 3.5. This is most closely approximated with 9 unit circles at a diameter ratio of 3.613 [5]. This yields a packing factor of 0.6895. With more testing and client feedback, the final choice will be selected all of factors above.

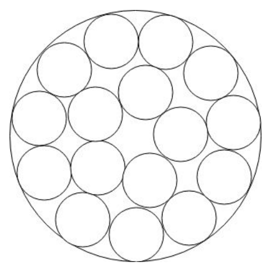

Figure 7 Approximate Example of Optimal Packing Orientation For 16 Circles

2.4.2 Lenses

The 110° viewing angle of our CREE XP-E2 LEDs is far too wide to directly couple with a fiber optic cable. For light to be transmitted inside a fiber optic cable, it needs to be at a near parallel angle to the cladding, or outer wall, of the cable so that it achieves total internal reflection and remains trapped within the cable. For the cable we used, this angle was given as α = 30° so for full acceptance, our light must be within a 60° angle [8]. This is illustrated in Figure 8.

Our solution was to use a PCB mountable lens, Carlco model 10193, and holder to act as a collimator and form the LED's output into a nearly parallel beam. When attached to the output of a CREE XP-E2 LED, this optic formed the light into a 20 mm diameter beam with half of its output within a minimal divergence of 8.2° [10]. Alone, however, this output is still far to diffuse since we are not using 20 mm diameter fiber optical cables. To correct for this, a plano-convex converging lens with 16.5 mm focal length and 20 mm diameter was affixed directly to the output of the Carlco optic. This lens was purchased on Amazon, item number B00XKXWEJ4, as glass options from optics manufactures were cost prohibitive.

With ideal parallel light entering an ideal convex lens, all of the light should be focused to an infinitely small spot one focal length away from the lens. However, since our light is not entirely parallel and lens not ideal, we measured a focal point of light with a diameter of ~7 mm. Simple trigonometry tell us that the angle this light makes is at most 62.4°, although the measured angle would be smaller, as non parallel incident light from the Carlco optic incident on the converging lens will converge at a point after the focal length. Due to higher powered glass lenses costing a factor of 20 more than our converging lens, this was deemed adequate for our project.

An illustration of our lens arrangement is shown below in Figure 9. The Carlco lens holder is perfectly centered on the LED on the driver via four manufactured holes in the PCB. The Carlco optic snaps into the holder and does not require alignment which will make assembling a large quantity of lenses easy. The plano-convex 20 mm converging lens aligns with the holder via the preexisting clips for the optic. The mounting plate is positioned exactly at one focal length, 16.5 mm, away from the converging lens and aligns the fiber optic cable perfectly with its focal point. Clear epoxy was used to secure the lens holder to the PCB and at the edges of the converging lens and the holder.

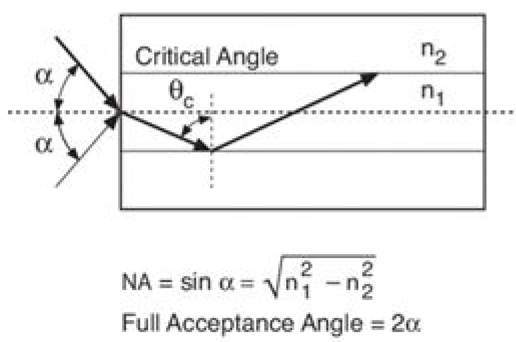

Figure 8 Acceptance Angle of Fiber Optic Cable [7]

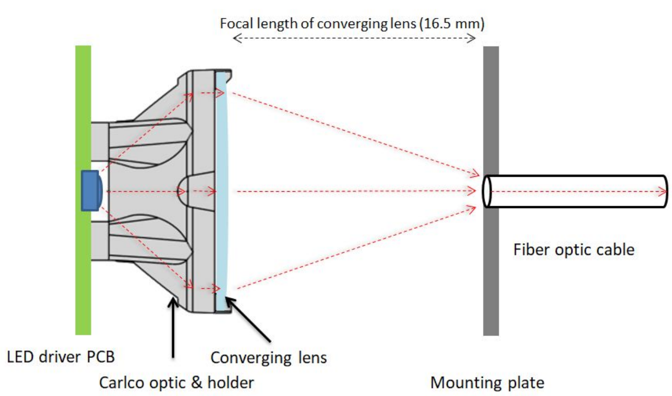

Figure 9 Arrangement of Lenses and Fiber Optic Cable[1]

[1] Not to scale

2.5 LED Driver

To keep our LED driver simple, improve robustness, and take advantage of our control chips, power BJTs were used to control the LED current. With the BJTs operating in the forward active mode, the collector current is equal to the base current multiplied by a fixed gain factor for the specific BJT. For our BJT, model D45H11, this value was around 60 Amps per Amp; to drive 1 Amp through the LED, the PWM chip needs to therefore sink only 15 mA of current which is controlled by a reference resistor [12,13]. Since our PWM generator chips have a variable current, this method provides excellent control over our LEDs. Furthermore, since the base of a BJT is often modeled as a diode, our PWM chips will be performing their intended function, driving an LED. The schematic of a single LED driver is shown in Figure 10, below.

Our heatsink is pictured below in Figure 11. It is mounted to the LED driver board using epoxy, as mounting holes were not added to the board for the heatsink. The small, 3.3 V fan was also mounted to the heatsink using glue. Future revisions of this board will include a proper mount for the sink, as well as a better fitting and replaceable fan.

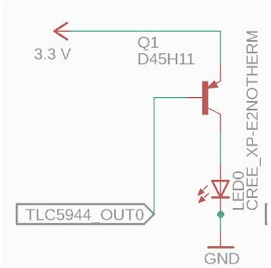

Figure 10 Single LED driver schematic

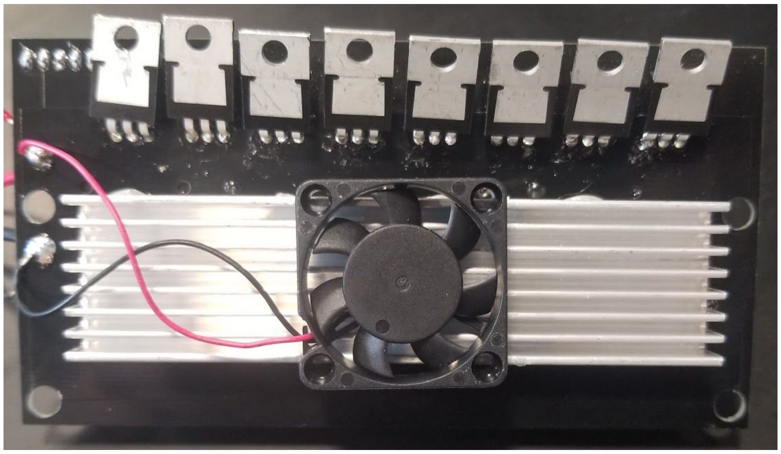

Figure 11 Heatsink and fan mounted to LED driver PCB

2.6 Power Supply

2.6.1 AC-DC Rectifier

Since our LED driver operates at the forward voltage of the LED plus the collector-emitter voltage of the BJT, our power supply could be chosen from the wide range of models available with a 3.3 Volt output. Simulation and testing showed that the collector-emitter voltage of our BJT at 1A current drive was around 0.3 Volts, so our power supply would need a slight variability of the output voltage to bring it to 3.6 Volts. Most 3.3 Volt supplies have this feature so we needed to identify a model that would be able to provide enough current for one section of LEDs, around 30 Amps, and fit within the space above the artwork. A supply manufactured by Mean Well, model RSP200-3.3, would suit our needs, however for testing a DC bench supply was sufficient and this power supply was not purchased.

2.6.2 Boost Converter

Since our control module and DMX receiver operate at 5 Volts, we designed a small boost converter to generate a 5 Volt, 1 Amp output from the 3.3 Volt input. A boost controller IC, model LTC3872, with integrated MOSFET gate driver was used to control the converter. Passive component sizing followed guidelines given in the manufacturer's data sheet for a 3.3 Volt to 5 Volt converter setup [11]. Although this is a low power converter, general switching regulator guidelines for PCB layout were followed to improve output voltage stability. Figures 12 and 13 show the schematic, as well as the PCB layout for this converter.

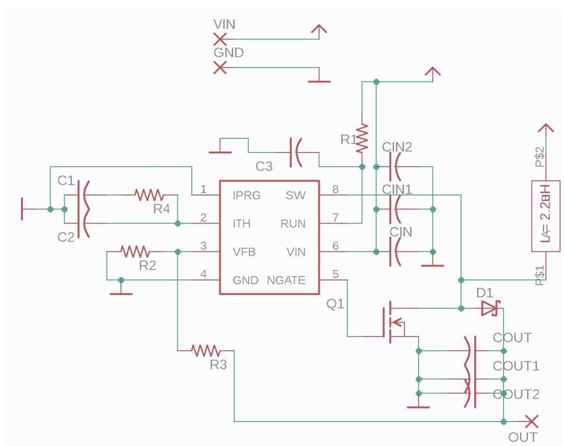

Figure 12 Boost converter schematic

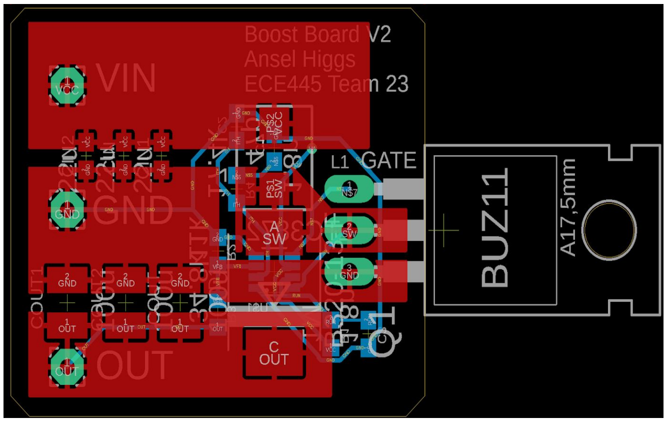

Figure 13 Boost converter PCB layout

3. Design Verification

3.1 DMX Testing

In-depth testing was done to get a more practical understanding of the DMX protocol. An oscilloscope was directly attached to the output of the DMX controller in order to establish a range for the idle, break, and mark after break periods. Testing gave the results of between 19-20ms for the idle period as shown in Figure 14. The break period was consistently 100µs and the mark after break period was consistently approximately 60µs, with no significant deviations observed as demonstrated in Figure 15. This test established the expected range of the idle period between data packets, ensuring that our microcontroller would not run into issues between receiving information from the RS485 bus and writing information to the shift registers contained in the PWM chips. One discrepancy is the mark after break period, which was much larger than what the protocol defines it to be (defined as 8µs but experimentally closer to 60µs).

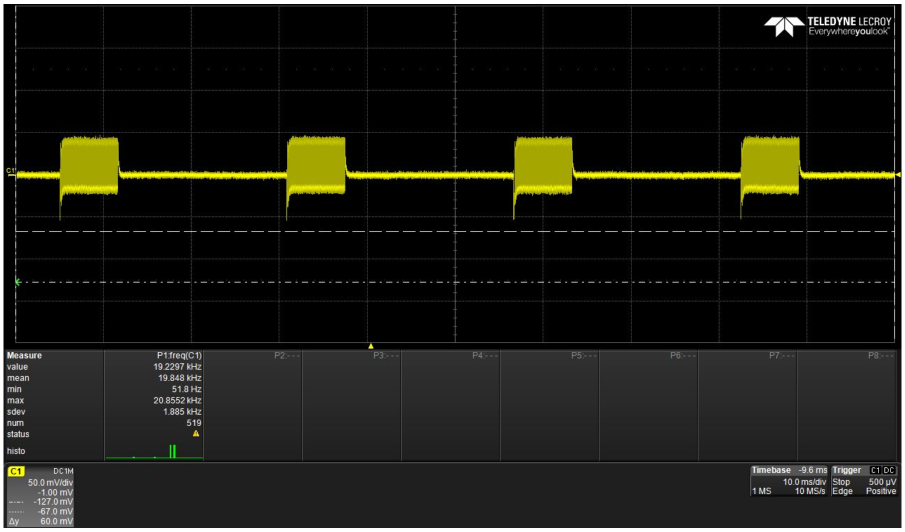

Figure 14 DMX Signal Showing Idle Periods In Between Data Packets

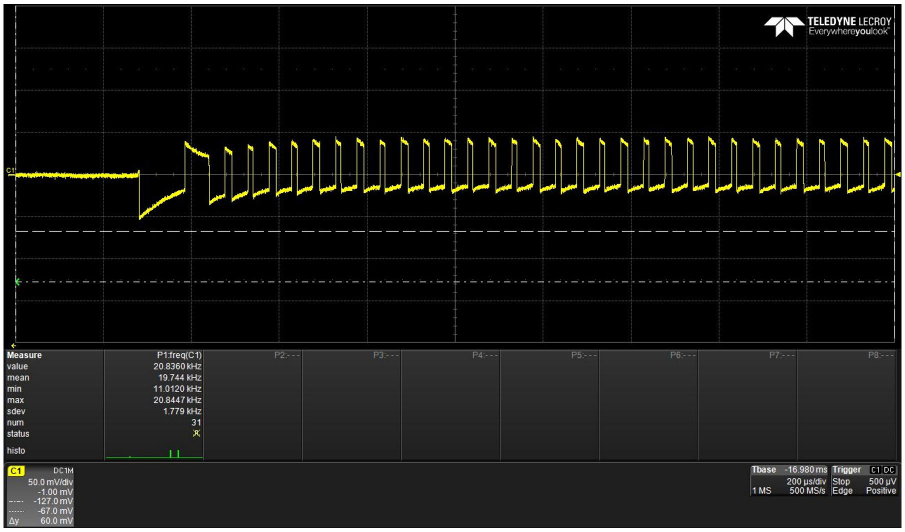

Figure 15 DMX Signal Closeup Showing Break, Mark After Break, and Data Packets

3.2 PCB Testing

3.2.1 Control Module Tests

We started with testing the PWM generator chip separately using an Arduino RedBoard to understand how the chip works. We soldered the chip to a breakout board, connected LEDs to the 16 constant current sinks outputs, and programmed it to alternate between the 16 LEDs by shifting in various data to the grayscale registers on the chip with 0.5 second delay. The LEDs were blinking as expected and we documented the control process in order to implement it on the ATmega328p. Testing the PWM generator using the oscilloscope was not efficient so we instead used LEDs to test.

After testing the output of the RS485 receiver and understanding the DMX protocol we connected said output to the USART0 unit on the ATmega328p and tested receiving frames in two ways: First, by blinking an LED if the microcontroller receives a specific frame value and set this value on the DMX controller to blink the LED. Second, by storing that value and send it serially to one of the I/O pins. Figure 16 shows a sequence of 8-bit data (01010000) repeatedly sent to the oscilloscope. Storing the DMX frames was inefficient for our project since the DMX packet takes a relatively long time. As a result, the microcontroller sends the data to the PWM generator registers immediately after receiving it.

After testing the PWM generators and the DMX receiver separately, we connected the microcontroller to the PWM generators on a breadboard via breakout boards and tested the unit by changing the brightness of LEDs connected to the PWM generators. We tested accuracy and consistency of each address by controlling each LED with a specific channel on the DMX controller (e.g. LED on output 1 controlled by channel 1).

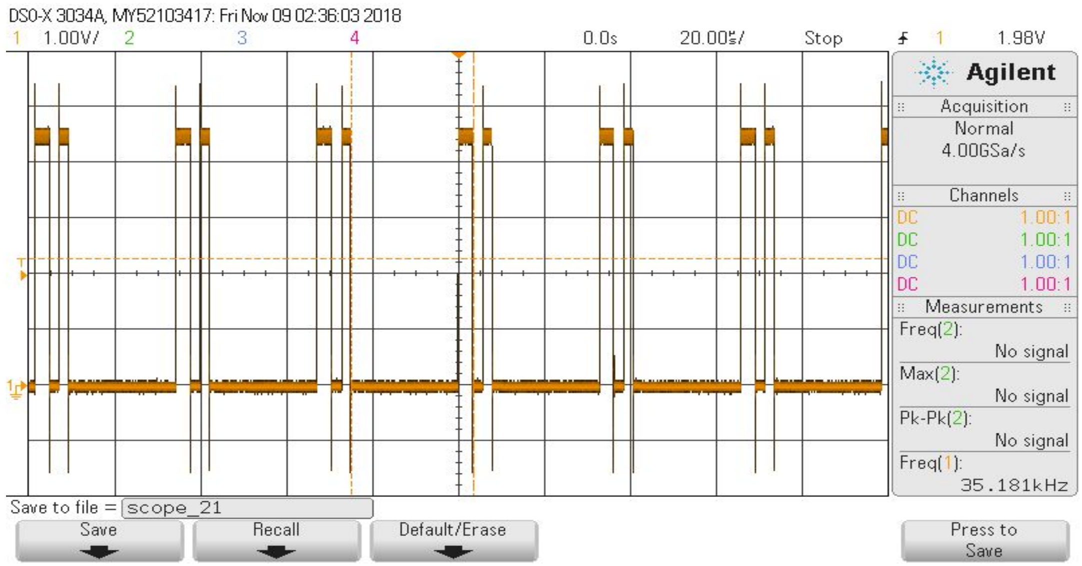

Figure 16 DMX Byte Data After USART0 Receiving

3.2.2 LED Driver Tests

To avoid uneven lighting, we tested the focused output of each individual LED on our board in order to ensure an acceptable level of uniformity. The lens pair was affixed to every LED and mounting plate was attached and aligned; all LEDs were driven at quarter intensity as to not overload the light meter. A 10 inch section of solid 8 mm fiber optic end glow cable was inserted into each hole and the light intensity was measured at the output of the cable using a Urceri MT-912 Light Meter. The results are outlined in Table 1. Our average output was 142 KLux, with a maximum of 19% deviation from the average output.

Table 1. Uniformity Testing Results for LEDs

LED #:	**1**	**2**	**3**	**4**	**5**	**6**	**7**	**8**
Output (KLux):	**148.0**	**150.0**	**125.0**	**154.1**	**158.8**	**131.3**	**127.2**	**147.4**

One of the most important tests for the LED driver was thermal dissipation when all LEDs are driven at maximum power. To verify this, the board was fully outfitted with lenses, the fiber optic mounting plate, heatsink, and fan. It was placed on the lab bench in the expected orientation for normal operation as seen in Figure 11. A DC supply was connected and the bases of all 8 BJTs were connected to ground with a resistor to drive approximately 15 mA through each and allow 8 A to flow through all of the LEDs. Temperature measurements were taken with an IR thermometer, model Zanmax 257730902-1 . A piece of Scotch tape was placed on the heatsink to correct for the emissivity of the reflective material as per the manufacturer's recommendation. After one hour of operation, LED and BJT temperature had stabilized at 181 ℉ and 153 ℉, respectively. The maximum temperature given by the manufacturer is 302 ℉ for both components, so we do not anticipate any longevity issues with our design. Table 2 summarizes these results.

Table 2 Thermal testing of LED driver board

Time (min.)	LED Temp. (℉)	BJT Temp. (℉)	Heatsink Temp. (℉)
0	104	83	100
1	130	102	120
5	163	120	152
10	172	123	158
15	175	151	162
30	177	141	164
45	179	151	165
60	180	150	165
75	180	150	164
90	180	153	164
105	180	150	162
120	181	149	161

3.2.3 Boost Converter Tests

The designed load of our boost converter is 1 A but for system implementation only the control board was connected to the converter. The observed load was much lower, around 100 mA. Although we did not experience any performance issues with the converter, we tested greater loads to verify stable operation. As stated in our design document, the boost converter must provide regulation at 5 V ± 5% at a 1 A load. This was verified by connecting the converter to an electronic load and setting the current to different values. The converter was powered by a DC bench supply connected to the LED driver board which shares power connections with the boost converter. At a 1 A load, the output voltage was within ± 5% during operation at a 3.6 V input. At a 3.3 V input, the output fell below our target range. However, since current of the DMX receiver and control board were measured to be around 100 mA each, our maximum expected load is closer to the data point taken at 0.5 A and our converter should operate within spec at this load. Figure 17 shows the results, demonstrating no discernable ripple in output voltage. There are high frequency spikes at each switching point although these are typical of switching regulators and could be eliminated by using a bank of lower valued output capacitors. Thes spikes caused no noticeable performance issues with any component on the control module PCB.

Table 3 Boost converter output at various loads

V_{in} (V)	I_{in} (A)	V_{out} (V)	I_{out} (A)	Efficiency	Ripple (mV)
3.3	0.915	4.97	0.52	86%	241
3.3	1.69	4.48	1.03	83%	248
3.3	1.86	3.26	1.5	80%	268
3.6	0.835	4.98	0.52	86%	261
3.6	1.627	4.78	1.03	84%	278
3.6	1.86	3.62	1.5	81%	278

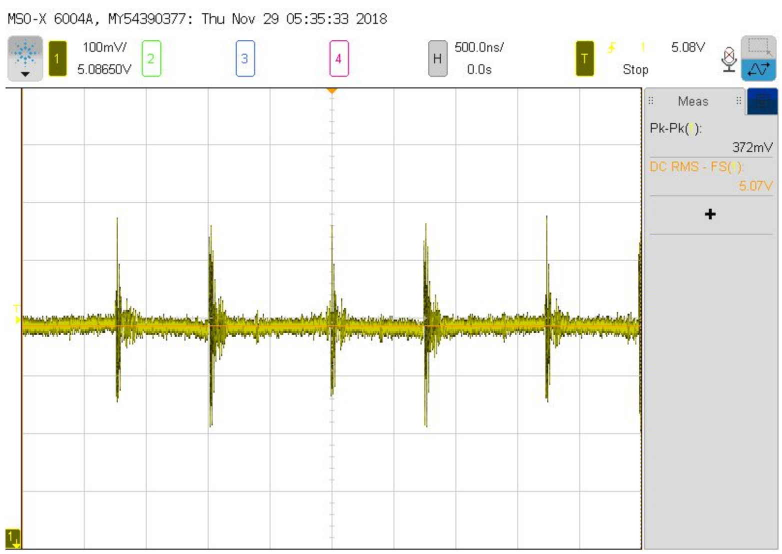

Figure 17 Boost converter output ripple at 3.3V in, 0.5 A load

3.3 Fiber Optic Testing

In order to ensure that there is sufficient light in order to illuminate the piece in various ambient lighting conditions, we tested the light transfer efficiency using a Urceri MT-912 Light Meter in order to measure the luminous flux per unit area at both the mounting plate hole used to connect the fiber optic cables and the ends of the fiber optic cable. The test was run at an LED voltage of 3.0 V as the rated 3.3 V resulted in luminous flux that exceeded what our equipment could measure. Table 4 shows the results of these tests.

Table 4 Lighting Transfer Efficiency Test Results

Cable Type:	0.75mm Stranded	1.5mm Solid	1.5 Stranded	8 mm Sideglow	2mm Stranded	2mm Braided
Input (kLux):	143.0	141.6	143.9	146.1	149.3	160.4
Output (kLux):	0.7011 x 32[2]	28.2	2.185 x 12[3]	68.2	33.6	20.6
% Efficiency	15.6	19.9	18.2	46.6	22.5	12.8

Our original requirement was >20% transfer efficiency, and we certainly have options that are acceptably near this number. The sideglow cable showed an impressively high transfer efficiency, which showcases just the significance of the packing factor loss discussed in Section 2.3.1. Of interest are the 0.75mm stranded and the 2mm braided cables. The 0.75mm stranded shows a very low transfer efficiency as the cable itself has a significantly smaller diameter compared to the 8mm hole, leading to a very large loss of light. The 2mm braided cable also showed a very low transfer efficiency due to the braided nature of the cables creating many bends that resulted in light loss down the length of the cable. Figure 18 shows the various cables that tested.

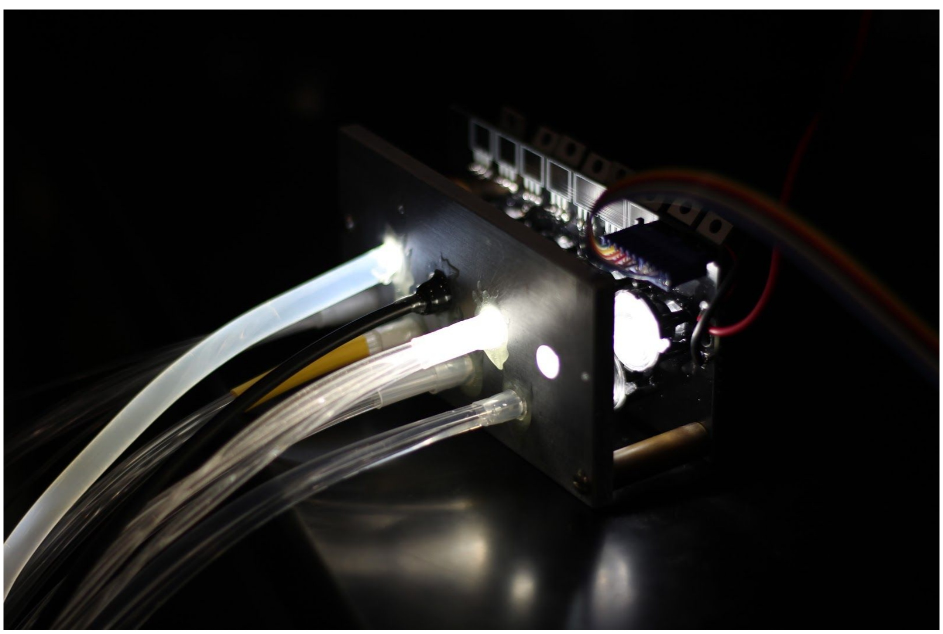

Figure 19 Fiber Optic Cables With Lighting. Top Left - Sideglow, Top Middle - 0.75mm Stranded, Top Right - 2.00mm Stranded

[2] A single strand was measured and then multiplied by the total number of strands present.
[3] See footnote 2, above.

4. Costs

4.1 Parts

The total estimated component costs are outlined in Table 5. This is a rough estimate, as final components such as the fiber optic cables have not been decided.

Table 5 Parts Costs

Part	Manufacturer	Retail Cost ($)	Bulk Purchase Cost ($)	Actual Cost ($)
DMX Controller/USB Adapter for Computer	Various	50	50	50
Wireless DMX Transmitter and Receiver	Donner	45	45	45
ATmega328p	Atmel	1.96	1.96	14
TLC5944 PWM Driver	Texas Instruments	2.81	2.52	36
RS-485 Receiver	Maxim Integrated	1.54	1.54	11
LEDs	Cree	1.25	1.06	223
PCB Lens & Mount	Carlco	1.63	1.39	292
Fiber Optic Cables	Various	~$200/100feet	~$200/100feet	1400
Power Supply	Mean Well	42	40	280
Optical Lenses	Amazon Madshop	0.80	0.80	168
Boost Converter Components	Various	18	8	56
Total	n/a	364.99	352.27	2575

4.2 Labor

Labor costs are estimated given an estimated $12/hour. We each put in roughly 100 hours, and using a 2.5x adjusting factor the final labor cost comes out to ~$9000. Due to the large scale nature of the final implementation of the design requiring a great deal of manual labor, we anticipate that to be a significant cost added on to the final cost of the project.

5. Conclusion

5.1 Results

The project came together with all components working as expected and in tandem. While functional, many improvements need to be made before a full scale implementation. Every part of our system has been vigorously tested and shown to be fully functional. While our circuit boards border on the fragile side, once installed they should not fall under much stress. The final fiber optic cable configuration has also not yet been decided as more tests on the actual artwork would be necessary before moving forward. Asides from small improvements and a final decision on the cables, we are fully confident that our design will come together to notably highlight the artwork.

5.2 Ethical Considerations

A significant safety issue is power. As we are working with voltage supplied from a wall socket there is significant potential for damage. To ensure that power is regulated at all times the power module will be well overrated for our intended maximum use situations. We also must ensure the weight of our design is not too great, as too much weight put onto the existing mounting bracket for the art installation will cause structural failure, which violates Article 1 of the IEEE code of ethics by risking the "safety, health, and welfare of the public"[6]. To ensure this does not happen, we will strictly adhere to the engineering design of the current predecessor and reinforce the mounting solution if required.

Article 1 of the IEEE code of ethics dictates that we "strive to comply with ethical design and sustainable development practices"[6]. We intend to adhere to this by ensuring that our design is as efficient as possible, taking advantage of the energy efficiency of LEDs compared to more traditional lighting elements. We will vigorously stress test our design in order to adhere to Article 9 of the IEEE code of ethics: "to avoid injuring others…"[6]. We also will establish clear communication with the end product user in order to be clear and ethical in our presentation of results as Article 3 of the IEEE code of ethics states [6].

5.3 Future Work

While the project is fully functional, several updates would be beneficial to the ease of production and quality of the final product. Updates to the PCBs are needed to make assembly easier and less prone to failure, such as a more reliable on-board fixture for the DMX input as well as headers for the control module outputs in order to accommodate standard ribbon cables for improved connections to the lighting module. Another area of potential improvement is the thermal performance. In the current iteration both a heatsink and fan are required in order to maintain acceptable temperature ranges. However, with a larger heatsink the fan may not be required which would be a significant improvement in terms of reliability. A larger budget would also enable exploration into more advanced lenses which would lead to improvements in terms of efficiency and a simplified construction.

References

[1] The DMX Packet, web page. Available at: https://web.archive.org/web/20170923181853/http://www.dmx512-online.com/packt.html . Accessed November 2018.

[2] *IPC-2221 Generic Standard on Printed Board Design,* Institute for Interconnecting and Packaging Electronic Circuits, Northbrook, Illinois, 1991

[3] *Microchip megaAVR,* datasheet, Microchip Technology, 2018. Available at: http://ww1.microchip.com/downloads/en/DeviceDoc/ATmega48A-PA-88A-PA-168A-PA-328-P-DS-DS40002061A.pdf

[4] Graham RL, Lubachevsky BD, Nurmela KJ,Ostergard PRJ. "Dense packings of congruent circles in a circle" *Discrete Math,* 1998; pp. 181.

[5] U. Pirl, "Der Mindestabstand von *n* in der Einheitskreisscheibe gelegenen Punkten", *Mathematische Nachrichten 40,* 1969, pp. 111-124.

[6] IEEE.org, "IEEE IEEE Code of Ethics", 2018. [Online]. Available: http://www.ieee.org/about/corporate/governance/p7-8.html. Accessed: 18 Sep. 2016.

[7] Fiber Optic Basics, Newport, website. Available at: https://www.newport.com/t/fiber-optic-basics. Accessed October 2018.

[8] Fiber Specifications & Photos, website. Available at: https://thefiberopticstore.com/faq/fiber-specifications-photos. Accessed October 2018.

[10] 20.0mm Narrow Spot Plain TIR (10193), website, Carlco Optics. Available at: http://www.carclo-optics.com/optic-10193. Accessed October 2018.

[11] Current Mode Boost DC/DC Controller, datasheet, Linear Technology, 2013. Available at: https://www.analog.com/media/en/technical-documentation/data-sheets/3872fc.pdf

[12] D44H Complementary Silicon Power Transistor, datasheet, On Semiconductors, 2014. Available at: https://www.onsemi.com/pub/Collateral/D44H-D.PDF

[13] 16-Channel, 12-Bit PWM LED Driver, datasheet, Texas Instruments, 2009. Available at: http://www.ti.com/lit/ds/symlink/tlc5944.pdf